# Self-consistent random-phase approximation at finite temperature within the Richardson model

Nguyen Dinh Dang*
*Heavy-Ion Nuclear Physics Laboratory, Nishina Center for Accelerator-Based Science, RIKEN, 2-1 Hirosawa, Wako City, 351-0198 Saitama, Japan*

Kosai Tanabe†
*Department of Physics, Saitama University, Sakura, Saitama 338-8570, Japan*
(Received 30 March 2005; revised manuscript received 24 May 2006; published 25 September 2006)

The self-consistent random-phase approximation (SCRPA) is extended to nonzero temperature. Within the SCRPA, the collective dynamics of nucleon pairs is built on the occupation numbers that deviate from the Fermi-Dirac distribution as a result of temperature-dependent correlations beyond the RPA. The equations for single-particle occupation numbers are derived using the method of the double-time Green's functions. The approach is applied to the Richardson model of pairing. The results of numerical calculations for energies of states and occupation numbers, as well as for the thermodynamic quantities such as the excitation energy and heat capacity of the system, are compared with those obtained within the conventional RPA and the perturbative thermal SCRPA and with the exact results. We find that, overall, the SCRPA offers a better agreement with the exact results.

DOI: 10.1103/PhysRevC.74.034326 PACS number(s): 21.60.Jz, 21.60.Cs, 21.90.+f

## I. INTRODUCTION

The random-phase approximation (RPA) is recognized as a powerful method for treating collective dynamics of small-amplitude motion in many-body systems. The recent development of the RPA includes its extension and improvement in two major directions. In the first direction, in order to describe highly excited nuclei (hot nuclei), the RPA was extended to finite temperature within the finite-temperature RPA (FT-RPA) [1]. Here, as in the standard statistical approach to nuclear study, the observables are replaced with averages over the statistical ensemble at a given temperature $T$, which corresponds to the excitation energy of the system. Traditionally, in the construction of the FT-RPA equation, the collective dynamics is built on thermodynamic states, whose single-particle occupation numbers are replaced with those given by the Fermi-Dirac distribution of noninteracting particles. The correctness of this substitution has been taken for granted for years, although it is clear that the single-particle occupation numbers in general should not follow the distribution of free particles because of the residual interaction.

In the second direction, the RPA was improved by taking into account dynamic correlations due to interactions or symmetries. The first step was the now well-known renormalized RPA (RRPA) [2], which was proposed as a remedy for the violation of the Pauli principle within the original RPA. As a further step in this direction, Dukelsky and Schuck proposed the method of self-consistent RPA (SCRPA) [3,4], which they successfully applied to the multilevel-pairing model with double degeneracy, known as the Richardson model (also called the picket-fence model) [4,5]. Compared to the RRPA, the SCRPA offers a significant improvement thanks to the inclusion of the screening corrections, which are the expectation values of the products of two pairing operators in the correlated ground state. It has been shown in Refs. [4,5] that these corrections overscreen the interaction, turning it from attraction to repulsion in agreement with the trend of the exact solution. As a result, the SCRPA yields solutions that are much closer to the exact ones than those given by the RPA for the correlation energy of the system with $N$ particles, as well as the energy of the first excited state of the system with $N + 2$ particles.

The goal of the present work is to merge these two directions by offering an extension of the SCRPA to finite temperature. The method proposed in this work takes into account nonperturbative correlations between particles, which are included in the traditional zero-temperature SCRPA, and extends the treatment of these correlations to finite temperature. With these SCRPA correlations taken into account, the distribution of single-particle occupation numbers naturally deviates from the Fermi-Dirac distribution for noninteracting fermions.

The typical incoherent particle-particle interactions and Pauli exchange terms are the main factors that do not permit the full dynamic decoupling of the RPA modes. Indeed, the time evolution of the RPA modes that follows from the commutators between single-particle operators and the Hamiltonian involve operators which are more complex than the single-particle ones. As a result, one obtains an infinite hierarchy of algebraic equations, which couple the single-particle propagator to the higher-order ones. The formal solution of this infinite set of equations yields a single-particle Green's function, which is different from that for free fermions by the presence of the mass operator. The latter includes the effects of coupling to complex (multiple-particle and multiple-hole) configurations, which in principle cannot be treated exactly. Therefore, approximations

*E-mail address: dang@riken.jp
†E-mail address: tanabe@phy.saitama-u.ac.jp

 

have to be made to close the hierarchy. In Ref. [3], e.g., the full single-particle Green's function is expressed in terms of a series of unperturbed single-particle propagators. The perturbation theory was used to cut the series up to the first order to obtain RRPA solutions [2]. This scheme was then applied to the Richardson model at finite temperature in Ref. [6], and referred to thereafter as the TSCRPA. The average over the statistical ensemble within the TSCRPA was restricted to terms that are linear in the perturbation series (the linear dissipative process). Moreover, in the numerical calculations, an additional approximation for the single-particle occupation number, called the extended quasiparticle approximation, was made, which neglects the imaginary part of the mass operator in the complex energy plane, assuming a negligible single-particle damping. This allowed the replacement of the Breit-Wigner-like kernel of the single-particle spectral intensity with a $\delta$ function, and permitted the exact expression for the single-particle occupation number to be expanded in power series in the frequency near the SCRPA solutions [7].

The approach of the present work is different from that of Refs. [3,6]. We extend the SCRPA to finite temperature using the equation of motion for the double-time Green's functions [8,9]. To close the hierarchy of equations, a standard decoupling approximation introduced by Bogolyubov and Tyablikov [8,9] is used to lower the order of double-time Green's functions. From this closed set of equations, one obtains the single-particle Green's function. The double-time Green's functions have three types, namely, the causal, retarded, and advanced ones. The causal double-time Green's function is the same as the Matsubara Green's function used in Ref. [6] if the latter is taken at the pure imaginary time $(\tau, \tau') = (it, it')$. It does not allow an analytic continuation into the complex energy plane; therefore, it is not suitable for the derivation of the single-particle damping. The advantage of the approach in the present paper is that it uses the retarded and advanced double-time Green's functions, which can be analytically continued into the complex energy plane. This analytic continuation yields a mass operator, whose imaginary part directly corresponds to the single-particle damping. This method is free from any constraints of perturbation theory.

In the present paper, we shall see if the conventional assumption, which replaces the single-particle occupation numbers within the FT-RPA with those given by the Fermi-Dirac distribution [1], is valid for practical applications. We shall also estimate the effect of correlations beyond RPA on the energies of excited states, occupation numbers, and thermodynamic quantities such as the excitation energy and heat capacity of the system. The Richardson model is used as a testing ground for all the derivations and numerical calculations. The results of calculations are compared with those given by the conventional FT-RPA, the TSCRPA, and the exact solution proposed in Ref. [10]. It is important to point out that although the RRPA and SCRPA have solutions at any values of the interaction parameter, in the region above the RPA collapsing point the energy of the ground state of the $(N+2)$-particle system relative to that of the $N$-particle system obtained within the SCRPA deviates significantly from the exact result, and the discrepancies increase with increasing interaction parameter [4,5,11]. In this region, a self-consistent quasiparticle RPA should be constructed based on the quasiparticle representation [12]. This is beyond the scope of the present paper. Therefore, all the numerical calculations in this work are limited to the region of the interaction parameter below the RPA collapsing point.

The paper is organized as follows. The outline of the Richardson model and its exact solution are discussed in Sec. II. The FT-RPA for this model is presented in Sec. III. The extension of SCRPA to finite temperature (FT-SCRPA) for the same model is carried out in Sec. IV. The results of numerical calculations are analyzed in Sec. V. The paper is summarized in the last section, where conclusions are drawn.

## II. THE RICHARDSON MODEL

The Richardson model under consideration in the present paper consists of $\Omega$ double-fold degenerate equidistant levels, containing $N$ fermions that interact via the pairing force with a strength given by the parameter $G$. The Hamiltonian for this model is [4,5,11]

$$H = \sum_{i=1}^{\Omega} (\epsilon_i - \lambda) N_i - G \sum_{i,j=1}^{\Omega} P_i^\dagger P_j, \tag{1}$$

where the particle-number operator $N_i$ and pairing operators $P_i^\dagger$, $P_i$ are given in terms of single-particle creation and destruction operators, $c_i^\dagger$ and $c_i$, as

$$N_i = c_i^\dagger c_i + c_{-i}^\dagger c_{-i}, \qquad P_i^\dagger = c_i^\dagger c_{-i}^\dagger, \qquad P_i = (P_i^\dagger)^\dagger. \tag{2}$$

These operators fulfill the following exact commutation relations:

$$[P_i, P_j^\dagger] = \delta_{ij}(1 - N_i), \tag{3}$$

$$[N_i, P_j^\dagger] = 2\delta_{ij} P_j^\dagger, \qquad [N_i, P_j] = -2\delta_{ij} P_j. \tag{4}$$

The single-particle energies take the values $\epsilon_k = k\epsilon$ with $k$ running over all $\Omega$ levels. Only the *ph*-symmetric case is considered here, which means that in the absence of interaction ($G = 0$), the lowest $\Omega_h = \Omega/2$ levels are occupied with $N = \Omega$ particles (two particles on each level). Numerating particle ($p$) and hole ($h$) levels from the levels closest to the Fermi surface, the particle and hole energies are equal to $\epsilon_p = \epsilon(\Omega/2 + p)$ and $\epsilon_h = \epsilon(\Omega/2 - h + 1)$, respectively, with $p(h) = 1, \ldots, \Omega/2$.

The pairing problem described by the Hamiltonian (1) can be solved exactly in several ways using the Richardson method [13], the infinite-dimensional algebras in Ref. [14], or the recently proposed exact-pairing method, which amounts to direct diagonalization in the Fock space [10]. The last option is used in the present paper because of its simplicity. The pairing Hamiltonian (1) does not affect unpaired particles, leaving them stationary on given levels. These partially occupied levels can serve as quantum numbers, called seniority. Each level $k$ can contain $s_k = 0$ or 1 unpaired particle. In the case of $s_k = 1$, the unpaired particle can be on either one of two time-conjugated orbitals, which doubles the degeneracy of the resulting many-body state. Hence, in the exact solution, the

pairing eigenstate with energy $e_k$ can be labeled with the set of seniorities $\{s_1, s_2, \ldots, s_\Omega\}$ and has the degeneracy $d_k = 2^s$, where the total seniority $s = \sum_k s_k$ is the total number of unpaired particles with the values $s = 0, 2, \ldots, \Omega$.

Having obtained the exact eigenvalues of the Richardson model, we can calculate the grand potential $\mathbf{\Omega}(\beta)$ and grand-partition function $\mathbf{Z}(\beta)$ of the grand-canonical ensemble at finite temperature $T = \beta^{-1}$ as [15,16]

$$\begin{aligned} \mathbf{\Omega}(\beta) &= -\beta^{-1}\ln Z(\beta), \\ \mathbf{Z}(\beta) &= \sum_{N,k} d_k(N)\exp\{-\beta[e_k(N) - \lambda N]\}, \end{aligned} \tag{5}$$

where $d_k(N)$ is the degeneracy for a given $N$-particle system. The average quantities such as the average particle number $\langle N\rangle$ and the total energy $\mathcal{E}(T)$ of the system are defined from the grand potential with the standard thermodynamic relations as

$$\begin{aligned} \langle N\rangle &= -\frac{\partial \mathbf{\Omega}(\beta)}{\partial\lambda} \\ &= \mathbf{Z}^{-1}(\beta)\sum_{N,k} N d_k(N)\exp\{-\beta[e_k(N) - \lambda N]\}, \end{aligned} \tag{6}$$

$$\begin{aligned} \mathcal{E}(T) = \frac{\partial[\beta\mathbf{\Omega}(\beta)]}{\partial\beta} &= \mathbf{Z}^{-1}\sum_{N,k} d_k(N)e_k(N) \\ &\times \exp\{-\beta[e_k(N) - \lambda N]\} - \lambda\langle N\rangle. \end{aligned} \tag{7}$$

In the statistical approaches to many-body systems such as the methods of single-particle and double-time Green's functions, it is convenient to use the grand-canonical ensemble because it often simplifies calculations [17], although it allows the particle number to fluctuate. Therefore, the use of the grand-canonical ensemble in finite nuclei requires the chemical potential $\lambda$ to be adjusted at each value of temperature $T$ to preserve the average particle number $\langle N\rangle$. If there is no summation over the varying particle numbers $N$ in Eqs. (5)–(7), one recovers the averages over the canonical ensemble, in which Eq. (6) becomes an identity.

In the comparison with the FT-RPA and FT-SCRPA solutions in this paper, we will refer to the thermodynamic quantities, which are obtained by giving the statistical weights within the canonical ensemble to the exact solutions, as the "exact" ones, having in mind the underlying thermodynamics put in them. We prefer to average the exact solutions over the canonical ensemble rather than in the grand-canonical one as the former does not allow the particle-number fluctuations. The comparison of the results obtained by averaging over the micro-canonical, canonical, and grand-canonical ensembles is an interesting subject, which deserves a separate study.

## III. FT-RPA

The FT-RPA equation and its derivation for particle-hole ($ph$) RPA can be found in many references, some of which are quoted in Ref. [1]. The present section outlines the FT-RPA for the particle-particle ($pp$) case within the Richardson model.

For the derivation of the FT-RPA equation, it is convenient to use the operators in the notation of Ref. [5]

$$M_p = N_p, \quad M_h = 2 - N_h, \quad Q_p^\dagger = P_p^\dagger, \quad Q_h = -P_h^\dagger, \tag{8}$$

whose exact commutation relations follow from Eqs. (3) and (4) as

$$[Q_p, Q_{p'}^\dagger] = \delta_{pp'}D_p, \qquad [Q_h, Q_{h'}^\dagger] = \delta_{hh'}D_h, \tag{9}$$

$$[M_i, Q_j^\dagger] = 2\delta_{ij}Q_j^\dagger, \qquad [M_i, Q_j] = -2\delta_{ij}Q_j, \tag{10}$$

where the operators $D_p$ and $D_h$ are defined as [11]

$$D_p = 1 - M_p = 1 - N_p, \quad D_h = 1 - M_h = N_h - 1. \tag{11}$$

Using the definitions (8) and (11) , the Hamiltonian (1) acquires a convenient form [5]

$$\begin{aligned} H = \epsilon\Omega^2/4 &+ \sum_{p=1}^{\Omega/2}(\epsilon_p - \lambda)M_p - \sum_{h=1}^{\Omega/2}(\epsilon_h - \lambda - G)M_h \\ &- G\sum_{pp'} Q_p^\dagger Q_{p'} - G\sum_{hh'} Q_h^\dagger Q_{h'} \\ &+ G\sum_{ph}(Q_p^\dagger Q_h^\dagger + Q_p Q_h). \end{aligned} \tag{12}$$

The FT-RPA equation is derived similarly to the RRPA [2]. The $pp$ case uses the pair-addition and pair-removal operators (phonons) in the form

$$\begin{aligned} A_\mu^\dagger &= \sum_p^{\Omega_p} X_p^\mu \overline{Q}_p^\dagger - \sum_h^{\Omega_h} Y_h^\mu \overline{Q}_h, \\ R_\lambda^\dagger &= \sum_h^{\Omega_h} X_h^\lambda \overline{Q}_h^\dagger - \sum_p^{\Omega_p} Y_p^\lambda \overline{Q}_p, \end{aligned} \tag{13}$$

respectively, where the notation

$$\overline{\mathcal{O}}_i^\dagger = \frac{\mathcal{O}_i^\dagger}{\sqrt{\langle D_i\rangle}}, \qquad \overline{\mathcal{O}}_i = \frac{\mathcal{O}_i}{\sqrt{\langle D_i\rangle}}, \qquad i = p, h \tag{14}$$

is used to denote the renormalized operators. Operator $A_\mu^\dagger$ transfers the states of the system with $N = \Omega$ particles to those of the system with $N + 2$ particles. Operator $R_\lambda^\dagger$ transfers the states of the $N$-particle system to those of the system with $N - 2$ particles.

Using Eq. (9), one can see that the ensemble average of the commutation relations for the pair-addition and pair-removal operators leads to the boson-type commutation relations

$$\langle[A_\mu, A_{\mu'}^\dagger]\rangle = \delta_{\mu\mu'}, \qquad \langle[R_\lambda, R_{\lambda'}^\dagger]\rangle = \delta_{\lambda\lambda'}, \tag{15}$$

provided the amplitudes $X$ and $Y$ satisfy the following normalization (orthogonality) conditions

$$\begin{aligned} \sum_p X_p^\mu X_p^{\mu'} - \sum_h Y_h^\mu Y_h^{\mu'} &= \delta_{\mu\mu'}, \\ \sum_h X_h^\lambda X_h^{\lambda'} - \sum_p Y_p^\lambda Y_p^{\lambda'} &= \delta_{\lambda\lambda'}, \\ \sum_p X_p^\mu Y_p^\lambda - \sum_h X_h^\lambda Y_h^\mu &= 0. \end{aligned} \tag{16}$$

The closure relations

$$\begin{aligned}\sum_{\mu} X_p^{\mu} X_{p'}^{\mu} - \sum_{\lambda} Y_p^{\lambda} Y_{p'}^{\lambda} &= \delta_{pp'},\\ \sum_{\lambda} X_h^{\lambda} X_{h'}^{\lambda} - \sum_{\mu} Y_h^{\mu} Y_{h'}^{\mu} &= \delta_{hh'},\\ \sum_{\lambda} X_h^{\lambda} Y_p^{\lambda} - \sum_{\mu} X_p^{\mu} Y_h^{\mu} &= 0,\end{aligned} \tag{17}$$

guarantee the following inverse transformation of Eqs. (13)

$$\begin{aligned}Q_p^{\dagger} &= \sqrt{\langle D_p\rangle}\left[\sum_{\mu} X_p^{\mu} A_{\mu}^{\dagger} + \sum_{\lambda} Y_p^{\lambda} R_{\lambda}\right],\\ Q_h &= \sqrt{\langle D_h\rangle}\left[\sum_{\lambda} X_h^{\lambda} R_{\lambda} + \sum_{\mu} Y_h^{\mu} A_{\mu}^{\dagger}\right].\end{aligned} \tag{18}$$

The FT-RPA equation is obtained in a standard way by linearizing the equation of motion or by using the double-time Green's functions method [1]. The derivation of the FT-RPA is based on the following three assumptions:

(i) In a way similar to the RPA, which calculates all the matrix elements within the Hartree-Fock (HF) ground state, the FT-RPA, while dealing with excited nuclei, replaces the state at some energy with the grand-canonical ensemble average of noninteracting fermions. As a result, the particle-occupation number $\langle N_i\rangle$ is approximated as

$$\langle N_i\rangle \equiv \langle c_i^{\dagger} c_i\rangle + \langle c_{-i}^{\dagger} c_{-i}\rangle \approx 2n_i^{\rm FD}, \tag{19}$$

where $n_i^{\rm FD}$ is the occupation number given by the Fermi-Dirac distribution

$$n_i^{\rm FD} = [e^{\beta(\epsilon_i-\lambda)} + 1]^{-1}. \tag{20}$$

In the statistical average within this approximation, the full Hamiltonian (1) is replaced with its single-particle part $H \to H_{\rm sp} = \sum_j (\epsilon_j - \lambda) c_j^{\dagger} c_j$ corresponding to the noninteracting Fermi gas.

Within the FT-RPA the temperature-dependent $\lambda$ is found from the equation

$$2\sum_{j=p,h} n_j^{\rm FD} = N, \tag{21}$$

which leads to $\langle {\rm HF}|N_p|{\rm HF}\rangle = 0$ and $\langle {\rm HF}|N_h|{\rm HF}\rangle = 2$ at $T = 0$. This means that the ground-state correlations beyond RPA are ignored. Within this assumption, the correlation factors $\langle D_i\rangle$ $(i = p, h)$ are approximated as

$$\langle D_p\rangle \approx 1 - 2n_p^{\rm FD}, \qquad \langle D_h\rangle \approx 2n_h^{\rm FD} - 1. \tag{22}$$

(ii) The number $\nu_\tau$ of addition (removal) phonons in the thermal equilibrium is set to zero, i.e.,

$$\nu_\mu = \langle A_\mu^{\dagger} A_\mu\rangle = 0, \qquad \nu_\lambda = \langle R_\lambda^{\dagger} R_\lambda\rangle = 0. \tag{23}$$

(iii) The screening corrections, which contain the thermal averages $\langle Q_i^{\dagger} Q_{i'}\rangle$ and $\langle Q_i^{\dagger} Q_{i'}^{\dagger}\rangle$, are also neglected.

Under the above assumptions, the matrix form of the standard FT-RPA equation for the addition modes is

$$\begin{pmatrix} A & B\\ -B & C\end{pmatrix}\begin{pmatrix} X^{\mu}\\ Y^{\mu}\end{pmatrix} = E_{\mu}\begin{pmatrix} X^{\mu}\\ Y^{\mu}\end{pmatrix}, \tag{24}$$

where the submatrices $A$, $B$, and $C$ have the same form as that of the RRPA ones [2,4,5,11]

$$\begin{aligned}A_{pp'}^{\rm FTRPA} &= \langle[\overline{Q}_p, [H, \overline{Q}_{p'}^{\dagger}]]\rangle\\ &= 2(\epsilon_p - \lambda)\delta_{pp'} - G\sqrt{\left(1 - 2n_p^{\rm FD}\right)\left(1 - 2n_{p'}^{\rm FD}\right)}, \quad (25)\\ B_{ph}^{\rm FTRPA} &= -\langle[\overline{Q}_p, [H, \overline{Q}_h]]\rangle\\ &= G\sqrt{\left(1 - 2n_p^{\rm FD}\right)\left(2n_h^{\rm FD} - 1\right)}, \quad (26)\\ C_{hh'}^{\rm FTRPA} &= -\langle[\overline{Q}_h, [H, \overline{Q}_{h'}^{\dagger}]]\rangle\\ &= 2(\epsilon_h - \lambda - G)\delta_{hh'} + G\sqrt{\left(2n_h^{\rm FD} - 1\right)\left(2n_{h'}^{\rm FD} - 1\right)}. \quad (27)\end{aligned}$$

At $T = 0$ the single-particle occupation numbers become $n_p^{\rm FD} = 0$ and $n_h^{\rm FD} = 1$, so one recovers the RPA submatrices.

## IV. EXTENSION OF SCRPA TO FINITE TEMPERATURE FOR RICHARDSON MODEL

### A. Derivation of FT-SCRPA equations

#### 1. *Equations for the screening corrections*

Compared to the RRPA, the advantage of the SCRPA is the inclusion of the screening corrections containing the nonzero expectation values of the products of two pair operators $\langle Q_p^{\dagger} Q_{p'}\rangle$, $\langle Q_h^{\dagger} Q_{h'}\rangle$ and $\langle Q_p Q_h\rangle$. After the solution of the RPA (SCRPA) equation [see, e.g., Eqs. (19)–(22) in Ref. [11]] or the FT-RPA equation (24) with submatrices (25)–(27), the model Hamiltonian can be represented as that of harmonic oscillators with $\Omega/2$ frequencies $E_\mu \equiv \mathcal{E}_\mu^{(N+2)} - \mathcal{E}_0^{(N)}$ given by the addition modes, and $\Omega/2$ frequencies $E_\lambda \equiv \mathcal{E}_0^{(N)} - \mathcal{E}_\lambda^{(N-2)}$ given by the removal modes, where $\mathcal{E}_0^{(N)}$ is the energy of the $N$-particle system in the RPA (SCRPA) ground state (at $T = 0$) or in thermal equilibrium (at $T \neq 0$). Together with Eq. (15) this means that the addition (removal) phonons are independent bosons. Therefore, the occupation numbers for these modes at $T \neq 0$ can be approximated by the Bose-Einstein distribution for noninteracting bosons with energies $E_\mu$ and $E_\lambda$, respectively. This gives

$$\begin{aligned}\nu_\mu &\equiv \langle A_\mu^{\dagger} A_\mu\rangle \approx (e^{\beta E_\mu} - 1)^{-1},\\ \nu_\lambda &\equiv \langle R_\lambda^{\dagger} R_\lambda\rangle \approx (e^{\beta E_\lambda} - 1)^{-1}.\end{aligned} \tag{28}$$

Here, as in the derivation of Eq. (20) for noninteracting fermions, the full Hamiltonian $H$ (1) is replaced with that describing the noninteracting Bose gas of phonons. Using assumption (28) and Eqs. (15)–(18), we obtain the screening corrections in the form

$$\begin{aligned}\langle Q_p^{\dagger} Q_{p'}\rangle = \langle P_p^{\dagger} P_{p'}\rangle &= \sqrt{\langle D_p\rangle\langle D_{p'}\rangle}\\ &\times\left[\sum_{\mu} X_p^{\mu} X_{p'}^{\mu}\nu_\mu + \sum_{\lambda} Y_p^{\lambda} Y_{p'}^{\lambda}(1 + \nu_\lambda)\right], \quad (29)\\ \langle Q_p Q_h\rangle = \langle Q_h^{\dagger} Q_p^{\dagger}\rangle = -\langle P_h^{\dagger} P_p\rangle = -\langle P_p^{\dagger} P_h\rangle &= \sqrt{\langle D_p\rangle\langle D_h\rangle}\\ &\times\left[\sum_{\lambda} X_h^{\lambda} Y_p^{\lambda}(1 + \nu_\lambda) + \sum_{\mu} X_p^{\mu} Y_h^{\mu}\nu_\mu\right], \quad (30)\end{aligned}$$

$$\langle Q^\dagger_h Q_{h'}\rangle = \langle P^\dagger_{h'} P_h\rangle - \delta_{hh'}\langle D_h\rangle = \sqrt{\langle D_h\rangle\langle D_{h'}\rangle} \times \left[\sum_\lambda X^\lambda_h X^\lambda_{h'} \nu_\lambda + \sum_\mu Y^\mu_h Y^\mu_{h'}(1+\nu_\mu)\right]. \quad (31)$$

These expressions are general because they are true for both *ph* asymmetric and symmetric cases. In the latter case, one recovers from them Eq. (22) of Ref. [6]. At $T = 0$, the phonon occupation numbers $\nu_\mu$ and $\nu_\lambda$ vanish, so one recovers from Eqs. (29)–(31) the expressions for the screening corrections within SCRPA [4,5,11]. The derivation of the FT-SCRPA submatrices $A$, $B$, and $C$ for the addition modes is carried out in a standard way by calculating the expectation values of the double commutators in Eqs. (25)–(27) making use of Eqs. (29)–(31) above. By factorizing $\langle D_i D_j\rangle \approx \langle D_i\rangle\langle D_j\rangle$, one obtains the FT-SCRPA submatrices, which have the same form as that of the SCRPA ones [4,5,11], i.e.,

$$A_{pp'} = 2\left\{\epsilon_p - \lambda + \frac{G}{\langle D_p\rangle}\left[\sum_{p''}\langle Q^\dagger_{p''} Q_p\rangle - \sum_{h''}\langle Q_p Q_{h''}\rangle\right]\right\} \times \delta_{pp'} - G\sqrt{\langle D_p\rangle\langle D_{p'}\rangle}, \quad (32)$$

$$B_{ph} = G\sqrt{\langle D_p\rangle\langle D_h\rangle}, \quad (33)$$

$$C_{hh'} = -2\left\{\epsilon_h - \lambda - G + \frac{G}{\langle D_h\rangle}\left[\sum_{h''}\langle Q^\dagger_h Q_{h''}\rangle - \sum_{p''}\langle Q^\dagger_{p''} Q^\dagger_h\rangle\right]\right\}\delta_{hh'} + G\sqrt{\langle D_h\rangle\langle D_{h'}\rangle}. \quad (34)$$

### 2. *Equation for the occupation number*

To self-consistently solve Eq. (24) with submatrices (32)–(34), we need to derive the equation for the occupation number $n_i$ $(i = n, h)$

$$n_p \equiv \tfrac{1}{2}\langle N_p\rangle, \qquad n_h \equiv \tfrac{1}{2}\langle N_h\rangle, \quad (35)$$

from which one can calculate the correlation factors $\langle D_i\rangle$ using Eq. (11).

For this purpose, we will employ the method of double-time Green's functions, which is briefly summarized as follows. The retarded double-time Green's function for two Heisenberg representations $\mathcal{A}(t)$ and $\mathcal{B}(t')$ of operators $\mathcal{A}$ and $\mathcal{B}$ is defined as [9]

$$G^r(t,t') = \langle\langle \mathcal{A}(t); \mathcal{B}(t')\rangle\rangle_r = -i\theta(t-t')\langle[\mathcal{A}(t), \mathcal{B}(t')]_\pm\rangle, \quad (36)$$

where $\theta(t-t')$ is the step function, $[\mathcal{A},\mathcal{B}]_+ = \{\mathcal{A},\mathcal{B}\} \equiv \mathcal{A}\mathcal{B} + \mathcal{B}\mathcal{A}$ if $\mathcal{A}$ and $\mathcal{B}$ are fermion operators, and $[\mathcal{A},\mathcal{B}]_- = [\mathcal{A},\mathcal{B}] \equiv \mathcal{A}\mathcal{B} - \mathcal{B}\mathcal{A}$ if they are boson operators. The advanced double-time Green's function $G^a(t,t')$ is obtained from the retarded one by replacing $-i\theta(t-t')$ with $i\theta(t'-t)$, while the causal double-time Green's function is given as

$$G^c(t,t') = -i\langle \mathcal{T}\mathcal{A}(t)\mathcal{B}(t')\rangle, \quad (37)$$

with $\mathcal{T}$ denoting the time-ordered product. The presence of the step function in the definitions of the retarded and advanced Green's functions allows them to be analytically continued into the complex energy plane [9]. The equation of motion is the same for all three types of Green's functions and is written in the form

$$i\frac{dG(t-t')}{dt} = \delta(t-t')\langle[\mathcal{A}(t), \mathcal{B}(t)]_\pm\rangle + \langle\langle[\mathcal{A}(t), H(t)]; \mathcal{B}(t')\rangle\rangle. \quad (38)$$

We now apply Eq. (38) for the retarded double-time Green's functions to derive the equation for the occupation number $n_i$. Since the latter is defined in terms of the quantity $\langle c^\dagger_{\pm i} c_{\pm i}\rangle$, it corresponds to the single-particle Green's function

$$G_i(t-t') = \langle\langle c_i(t); c^\dagger_i(t')\rangle\rangle. \quad (39)$$

Calculating the exact commutators at the right-hand side (rhs) of Eq. (38) for $G_i(t-t')$ (39) and the Hamiltonian (1), we obtain the exact equation of motion for $G_i(t-t')$

$$i\frac{dG_i(t-t')}{dt} = \delta(t-t') + (\epsilon_i - \lambda)G_i(t-t') - G\sum_j \Gamma_{ij}(t-t'), \quad (40)$$

where $\Gamma_{ij}(t-t')$ denotes the double-time Green's function

$$\Gamma_{ij} = \langle\langle c^\dagger_{-i}(t)P_j(t); c^\dagger_i(t')\rangle\rangle, \quad (41)$$

which is a higher-order one compared to $G_i(t-t')$. We derive for function $\Gamma_{ij}$ an equation of motion in the same way using Eq. (38) and Hamiltonian (1). The exact result yields

$$i\frac{d\Gamma_{ij}(t-t')}{dt} = \delta(t-t')n_j\delta_{ij} + (2\epsilon_j - \epsilon_i - \lambda)\Gamma_{ij}(t-t') + G\sum_{j'}\{\langle\langle P^\dagger_{j'}(t)c_i(t)P_j(t); c^\dagger_i(t')\rangle\rangle - \langle\langle c^\dagger_{-i}(t)[1-N_j(t)]P_{j'}(t); c^\dagger_i(t')\rangle\rangle\}. \quad (42)$$

Different from the instantaneous approximation in Refs. [3,6], Eqs. (40) and (42) are obtained here without neglecting any part of the model Hamiltonian (1). To lower the order of the two Green's functions in the last term at the rhs of Eq. (42), we apply the Bogolyubov-Tyablikov decoupling of the higher-order Green's functions by pairing off operators referring to the same times [8,9], namely,

$$\langle\langle P^\dagger_{j'}(t)c_i(t)P_j(t); c^\dagger_i(t')\rangle\rangle = \langle\langle P^\dagger_{j'}(t)P_j(t)c_i(t); c^\dagger_i(t')\rangle\rangle \approx \langle P^\dagger_{j'}P_j\rangle G_i(t-t'), \quad (43)$$

$$\langle\langle c^\dagger_{-i}(t)[1-N_j(t)]P_{j'}(t); c^\dagger_i(t')\rangle\rangle \approx (1-\langle N_j\rangle)\Gamma_{ij'}(t-t'). \quad (44)$$

This decoupling is the simplest one for our present task as it is limited to lowest-order Green's functions and factors out the screening corrections $\langle P^\dagger_{j'}P_j\rangle$ as well as the correlation factors $(1-\langle N_j\rangle)$. Substituting the expressions at the rhs of Eqs. (43) and (44) for the terms in the last sum at the rhs of Eq. (42), and taking the Fourier transforms of Eqs. (38) and (42), we obtain the following closed set of equations for Green's functions

$G_i(E)$ and $\Gamma_{ij}(E)$ in the energy plane $E$

$$(E-\epsilon_i+\lambda)G_i(E)+G\mathcal{G}_i(E)=\frac{1}{2\pi}, \tag{45}$$

$$(E-2\epsilon_j+\epsilon_i+\lambda)\Gamma_{ij}(E)+G(1-2n_j)\mathcal{G}_i(E) - G\mathcal{M}_jG_i(E)=\frac{1}{2\pi}n_j\delta_{ij}, \tag{46}$$

where $E$, in general, is complex. In Eqs. (45) and (46), the first one of which is still exact, the following shorthand notations are used:

$$\mathcal{G}_i(E)\equiv\sum_j\Gamma_{ij}(E),\qquad \mathcal{M}_j\equiv\sum_{j'}\langle P^\dagger_{j'}P_j\rangle. \tag{47}$$

Extracting $\mathcal{G}_i(E)$ from Eq. (46) and inserting it into Eq. (45), one obtains the expression of $\Gamma_{ij}(E)$ in terms of $G_i(E)$ as

$$\Gamma_{ij}(E)=\frac{1-2n_j}{E-2\epsilon_j+\epsilon_i+\lambda}\left[\left(E-\epsilon_i+\lambda+\frac{G\mathcal{M}_j}{1-2n_j}\right)\times G_i(E)-\frac{1}{2\pi}\left(1-\frac{n_j\delta_{ij}}{1-2n_j}\right)\right], \tag{48}$$

where $(ij)=(pp')$ or $(hh')$. Using Eq. (48) to calculate $\mathcal{G}_i(E)$ and inserting the result into Eq. (45), we finally obtain the explicit form of function $G_i(E)$ as

$$G_i(E)=\frac{1}{2\pi}\frac{1}{E-\epsilon_i+\lambda+\Phi_i(E)}, \tag{49}$$

where the mass operator $\Phi_i(E)$ has the form

$$\Phi_i(E)=\left(n_i+G\sum_j\frac{\mathcal{M}_j}{E-2\epsilon_j+\epsilon_i+\lambda}\right)\times\left(\frac{1}{G}+\sum_{j\neq i}\frac{1-2n_j}{E-2\epsilon_j+\epsilon_i+\lambda}-\frac{n_i}{E-\epsilon_i+\lambda}\right)^{-1}, \tag{50}$$

$(i,j)=(p,p'),\ (h,h').$

The presence of the mass operator $\Phi_i(E)$ in the Green's function $G_i(E)$ in Eq. (49) shows the difference between the single-particle propagation and that of noninteracting single particles. Hence the functional form of the occupation number $n_i$ is not the one given by the Fermi-Dirac distribution (20) either.

Knowing the Green's function $G_i(E)$ (49), we find the time-correlation function

$$\mathcal{F}_i(t-t')\equiv\langle c_i^\dagger(t')c_i(t)\rangle=\int_{-\infty}^{\infty}J_i(\omega)e^{-i\omega(t-t')}d\omega \tag{51}$$

from the relation of the spectral intensity $J_i(\omega)$ ($\omega$ real) with the Green's functions:

$$J_i(\omega)=i[G_i(\omega+i\varepsilon)-G_i(\omega-i\varepsilon)](e^{\beta\omega}+1)^{-1},\quad(\varepsilon\to0). \tag{52}$$

The explicit expression for the spectral intensity is derived from Eqs. (49) and (52) in the form [8]

$$J_i(\omega)=\frac{1}{\pi}\frac{\gamma_i(\omega)(e^{\beta\omega}+1)^{-1}}{[\omega-\epsilon_i+\lambda+\Phi_i(\omega)]^2+\gamma_i^2(\omega)}, \tag{53}$$

where $\gamma_i(\omega)$ is the single-particle damping, which is obtained as the imaginary part of the analytic continuation of the mass operator $\Phi_i(E)$ into the complex-energy plane $E=\omega\pm i\varepsilon$, namely,

$$\Phi_i(\omega\pm i\varepsilon)=\Phi_i(\omega)\mp i\gamma_i(\omega). \tag{54}$$

After some algebra, we find from Eqs. (50) and (54)

$$\gamma_i(\omega)\equiv\Im m[\Phi_i(\omega\pm i\varepsilon)]=\frac{\boldsymbol{\mathcal{B}}_i(\omega)\mathcal{C}_i(\omega)-\boldsymbol{\mathcal{A}}_i(\omega)\mathcal{D}_i(\omega)}{\mathcal{C}_i^2(\omega)+\mathcal{D}_i^2(\omega)}, \tag{55}$$

where

$$\begin{aligned}\boldsymbol{\mathcal{A}}_i(\omega)&=n_i+G\sum_j\mathcal{M}_j\mathcal{P}\frac{1}{\omega-2\epsilon_j+\epsilon_i+\lambda},\\ \boldsymbol{\mathcal{B}}_i(\omega)&=\pi G\sum_j\mathcal{M}_j\delta(\omega-2\epsilon_j+\epsilon_i+\lambda),\\ \boldsymbol{\mathcal{C}}_i(\omega)&=\frac{1}{G}+\sum_{j\neq i}(1-2n_j)\mathcal{P}\frac{1}{\omega-2\epsilon_j+\epsilon_i+\lambda}-n_i\mathcal{P}\frac{1}{\omega-\epsilon_i+\lambda},\\ \boldsymbol{\mathcal{D}}_i(\omega)&=\pi\left[\sum_{j\neq i}(1-2n_j)\delta(\omega-2\epsilon_j+\epsilon_i+\lambda)-n_i\delta(\omega-\epsilon_i+\lambda)\right].\end{aligned} \tag{56}$$

The symbol $\mathcal{P}$ in Eqs. (56) denotes the principal value of the corresponding integral. The derivation of Eqs. (54)–(56) has used the identity

$$\frac{1}{E-\omega\pm i\varepsilon}=\mathcal{P}\frac{1}{E-\omega}\mp i\pi\delta(E-\omega), \tag{57}$$

where $\varepsilon\to0$. In practical calculations of the damping $\gamma_i(\omega)$ based on Eqs. (55) and (56) the following presentation of the $\delta$ function is used

$$\delta(x)=\frac{1}{2\pi i}\left(\frac{1}{x-i\varepsilon}-\frac{1}{x+i\varepsilon}\right), \tag{58}$$

with a sufficiently small $\varepsilon$. The $t=t'$ limit of the time-correlation function (51) gives the final equation for the single-particle occupation number $n_i$, i.e.,

$$n_i=\frac{1}{\pi}\int_{-\infty}^{\infty}\frac{\gamma_i(\omega)(e^{\beta\omega}+1)^{-1}}{[\omega-\epsilon_i+\lambda+\Phi_i(\omega)]^2+\gamma_i^2(\omega)}d\omega. \tag{59}$$

Since the single-particle damping (55) is determined by the screening corrections $\mathcal{M}_j\equiv\sum_{j'}\langle P^\dagger_{j'}P_i\rangle$, the omission of the screening corrections is equivalent to neglecting the damping, i.e., setting $\gamma_i(\omega)\to0$. In this case, the expression under the integral at the rhs of Eq. (59) can be approximated with $(e^{\beta\omega}+1)^{-1}\delta(\omega-\widetilde{\epsilon}_i)$; hence, $n_i\to n_i^{\rm FD}(\widetilde{\epsilon}_i)$, i.e., one recovers the Fermi-Dirac distribution of noninteracting fermions at shifted energies $\epsilon_i'\equiv\widetilde{\epsilon}_i+\lambda$ given by Eq. (A2) of the Appendix VI. Neglecting the mass operator $\Phi_i(E)$ in Eq. (49), one recovers from Eq. (59) the Fermi-Dirac distribution of free fermions at energies $\epsilon_i$.

The set of Eq. (24) with submatrices (32)–(34), Eqs. (28)–(31), (50), (55), and (59) should be solved self-consistently with the normalization condition (16) at each value of temperature. They form the FT-SCRPA equations, whose solutions define the $X^\mu$, $Y^\mu$ amplitudes and the energies $E_\mu$ for the addition mode as functions of temperature. In practical calculations, the FT-SCRPA equations are solved by iteration as follows:

(i) The starting values for $n_i$ are assumed to be $n_i^{\rm FD}$.
(ii) They are used as inputs to solve the SCRPA equations (24) with submatrices (32)–(34).
(iii) The solution of the SCRPA equation yields the correlation factors $\langle D_i\rangle$ following the recipe of Ref. [5], from which one obtains $\bar{n}_i$ using Eqs. (11) and (35).
(iv) Using the obtained $\bar{n}_i$, one calculates $\mathcal{M}_j$ (47), $\Phi_i(\omega)$ (50), and $\gamma_i(\omega)$ (55).
(v) Using these quantities, one calculates the occupation number $n_i$ from Eq. (59).
(vi) Using the obtained $n_i$ as inputs, one goes back to step (ii) and repeats the iteration until the required precision for convergence is achieved.

### B. Pair-transition probability, energy-weighted sum of strengths, and excitation energy

We derive here the expressions for the quantities which reflect the evolution of the system at $T \neq 0$. At zero temperature, the probability of the transition generated by the pairing operator

$$K = \sum_p Q_p^\dagger - \sum_h Q_h + \text{h.c.} \tag{60}$$

between the ground state $|0\rangle$ of the $N$-particle system and the excited state $|\mu\rangle$ of a system with $N+2$ particles is proportional to the square $B(\mu, T=0)$ of the matrix element $\langle\mu|K|0\rangle$, i.e.,

$$B(\mu, T=0) \equiv |\langle\mu|K|0\rangle|^2 = |\langle 0|A_\mu K|0\rangle|^2. \tag{61}$$

At $T \neq 0$, replacing the expectation value $\langle 0|\ldots|0\rangle$ in the ground state at the rhs of Eq. (61) with the statistical ensemble average, $\langle\ldots\rangle$, as well as using Eqs. (13), (16), (17), and (29)–(31), we obtain

$$B(\mu, T) = \left| \sum_p \sqrt{\langle D_p\rangle} X_p^\mu - \sum_h \sqrt{\langle D_h\rangle} Y_h^\mu \right|^2. \tag{62}$$

Using Eq. (3) and the decoupling within FT-RPA

$$\langle P_i^\dagger P_{i'}\rangle = \langle c_i^\dagger c_{-i}^\dagger c_{-i'} c_{i'}\rangle = \langle c_i^\dagger c_{i'} c_{-i}^\dagger c_{-i'}\rangle \approx \delta_{ii'}\left(n_i^{\rm FD}\right)^2, \tag{63}$$

we estimate the corresponding value within the FT-RPA as

$$B(\mu, T)_{\rm FTRPA} = \left| \sum_p \left( \sqrt{1-2n_p^{\rm FD}} - \frac{\left(n_p^{\rm FD}\right)^2}{\sqrt{1-2n_p^{\rm FD}}} \right) X_p^\mu - \sum_h \frac{\left(n_h^{\rm FD}\right)^2}{\sqrt{2n_h^{\rm FD}-1}} Y_h^\mu \right|^2. \tag{64}$$

The energy-weighted sum of strengths (EWSS) is proportional to the quantity

$$S_1 = \sum_\mu E_\mu B(\mu, T). \tag{65}$$

The Landau splitting (spreading) of the distribution is calculated as

$$\sigma = \sqrt{\prec E^2 \succ - \prec E \succ^2}, \quad \prec E^k \succ = \frac{\sum_\mu E_\mu^k B(\mu, T)}{\sum_\mu B(\mu, T)}. \tag{66}$$

The excitation energy of the system is defined as

$$E^* = \mathcal{E}(T) - \mathcal{E}(0) \tag{67}$$

where $\mathcal{E}(T)$ is the total energy of the system at temperature $T$, which is obtained by averaging the Hamiltonian (12) in the form

$$\mathcal{E}(T) \equiv \langle H\rangle = \sum_p^{\Omega_p} (\epsilon_p - \lambda)(1 - \langle D_p\rangle) - \sum_h^{\Omega_h} (\epsilon_h - \lambda - G)(1 - \langle D_h\rangle) - G\left[ \sum_{pp'} \langle Q_p^\dagger Q_{p'}\rangle + \sum_{hh'} \langle Q_h^\dagger Q_{h'}\rangle - 2\sum_{ph} \langle Q_p^\dagger Q_h^\dagger\rangle \right] - \frac{\epsilon\Omega^2}{4}. \tag{68}$$

The value $\mathcal{E}(0)$ of this energy at $T=0$ is nothing but the energy in the ground state of the $N$-particle system (i.e., $\mathcal{E}_0^{(N)}$ at $T=0$), obtained in Ref. [5].

For comparison, the excitation energy within the FT-RPA is calculated by taking the ensemble average of Hamiltonian (1) under assumption (i), and by using the inverse transformation (18). The result yields

$$E^*_{\rm FTRPA} = \mathcal{E}(T)_{\rm FTRPA} - \mathcal{E}(0)_{\rm FTRPA}, \tag{69}$$

where

$$\mathcal{E}(T)_{\rm FTRPA} = 2\sum_{j=p,h} (\epsilon_j - \lambda) n_j^{\rm FD} - G\sum_h \left(2n_h^{\rm FD} - 1\right) - G\left[ \sum_{pp'} \sqrt{\left(1-2n_p^{\rm FD}\right)\left(1-2n_{p'}^{\rm FD}\right)} \sum_\lambda Y_p^\lambda Y_{p'}^\lambda + \sum_{hh'} \sqrt{\left(2n_h^{\rm FD}-1\right)\left(2n_{h'}^{\rm FD}-1\right)} \sum_\mu Y_h^\mu Y_{h'}^\mu - 2\sum_{ph} \sqrt{\left(1-2n_p^{\rm FD}\right)\left(2n_h^{\rm FD}-1\right)} \sum_\lambda X_h^\lambda Y_p^\lambda \right]. \tag{70}$$

The correlation energy is calculated as the difference between the total energy $\mathcal{E}(T)$ and the HF energy $\mathcal{E}_{\rm HF}$, namely,

$$E_{\rm cor} = \mathcal{E}(T) - \mathcal{E}_{\rm HF}, \tag{71}$$

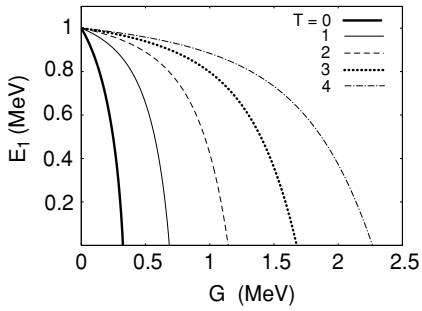


FIG. 1. Energy of the ground state (thermal equilibrium) of the system with $\Omega = 10$ levels and $N = 12$ particles relative to that of the system with $\Omega = N = 10$ obtained within the RPA as a function of interaction parameter $G$ at several temperatures $T$ (in MeV) shown by the numbers in the figure.

where

$$\mathcal{E}_{\rm HF} = 2\sum_j (\epsilon_j - \lambda) n_j^{\rm FD} - G\sum_{j<j'} n_j^{\rm FD} n_{j'}^{\rm FD}. \tag{72}$$

Finally, the specific heat is calculated in a standard way [1] as

$$C = \frac{\partial \mathcal{E}(T)}{\partial T}. \tag{73}$$

## V. RESULTS OF NUMERICAL CALCULATIONS

### A. Ingredients of numerical calculations

The FT-RPA and FT-SCRPA equations were solved numerically at $T \neq 0$ for additional modes within the Richardson model with the level distance $\epsilon = 1$ MeV at several values of $N$. In Sec. V B we choose to discuss in detail the results obtained with $N = 10$. For the comparison with the perturbative approach in Sec. V C the results of calculations obtained for $N = 6$ and 8 are also analyzed. Since all calculations are carried out at finite $T$, in the rest of the paper we will omit the prefix FT by addressing the FT-RPA and FT-SCRPA simply as RPA and SCRPA, respectively.

The value of $G_{\rm crit}$, at which the RPA collapses, does not stay constant but increases with $T$ from around 0.34 MeV at $T = 0$ [4,5,11] to around 2.25 MeV at $T = 4$ MeV as shown in Fig. 1. As we aim to follow the evolution of the RPA and SCRPA solutions as functions of $T$ starting from $T = 0$, we prefer to choose the values of $G$ within a range where the RPA solutions exist at any $T$, namely, up to $G_{\rm crit}^{\rm RPA}$, which is the value of $G_{\rm crit}$ obtained within the RPA at $T = 0$. In this region, the BCS has no solution. [1] The calculations are carried out using a smoothing parameter $\varepsilon = 0.5$ MeV. We did not find significant differences for all quantities considered in this paper when carrying out the calculations using different values of $\varepsilon$ between $0.1 \leqslant \varepsilon \leqslant 1$ MeV.

As the RPA and SCRPA preserve the seniority, in comparing the energies of the addition modes with the exact results we use for the latter the energies of the excited states at a given seniority in the system with $N + 2$ particles relative to the thermal equilibrium (or the ground state if $T = 0$) of the system with $N$ particles at the same seniority. These exact energies are found from Eq. (7) as

$$E_i = \mathcal{E}^{(N+2)}(i) - \mathcal{E}^{(N)}(i) = \langle E(N+2)\rangle_i - \langle E(N)\rangle_i - 2\lambda, \tag{74}$$

where $i = 1, 2, \ldots$ correspond to the states with total seniorities $s = 0, 2, 4, \ldots$, and the temperature-dependent chemical potential is defined as $\lambda = \frac{1}{2}[\langle E(N+2)\rangle - \langle E(N)\rangle]$.

### B. Analysis of numerical results

It is worth mentioning that the limitation of the configuration space leads to the Schottky anomaly [18], according to which the heat capacity increases with $T$ only up to a certain temperature, then decreases as $T$ increases further. With $\Omega = N = 10$, the heat capacities obtained within the RPA and SCRPA reach the maximum at $T_{\rm c} \sim 1.2$–$1.3$ MeV. The bump at $T < 0.25$ MeV is caused by the limitation of the energy space within the RPA and SCRPA, while no bump is seen in the exact heat capacity. This effect has been discussed in the context of the ground-state rotational band in Refs. [18,19], where the eigenvalues depend on the angular momentum $J$ and the band number $n$ rather than on $\mathcal{N}_j$ and $s_j$ as in the present model. Figure 2 shows that at $T \leqslant T_{\rm c}$ the heat capacities

[1] The value of $G_{\rm crit}^{\rm RPA}$ coincides with that of $G_{\rm crit}^{\rm BCS}$ if the self-energy term $-Gv_i^2$ is included in the single-particle energy $\epsilon_i' = \epsilon_i - Gv_i^2$ in solving the BCS equation. Otherwise $G_{\rm crit}^{\rm BCS} < G_{\rm crit}^{\rm RPA}$ (see Ref. [12]). In the present model with $N = 10$, if the self-energy term is neglected, we obtain $G_{\rm crit}^{\rm BCS} \simeq 0.28$ MeV at $T = 0$.

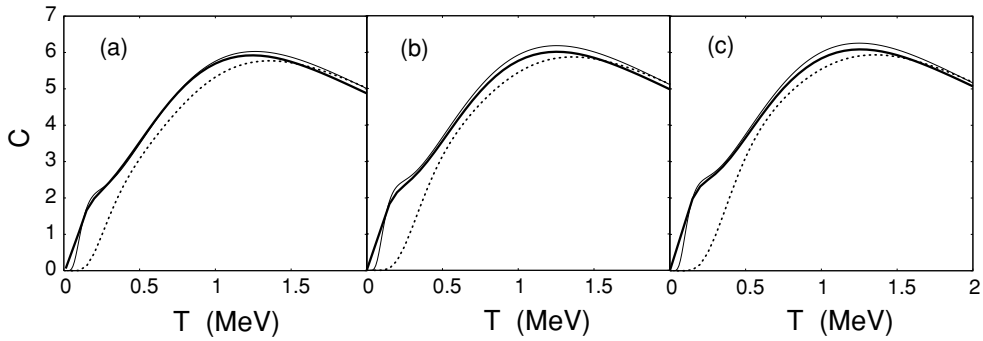


FIG. 2. Heat capacity of the $\Omega = N = 10$ system as a function of temperature $T$. Thin solid, thick solid, and dotted lines show the RPA, SCRPA, and exact results, respectively. Panels (a)–(c) correspond to the results obtained at $G = 0.1$, 0.2, and 0.25 MeV, respectively.

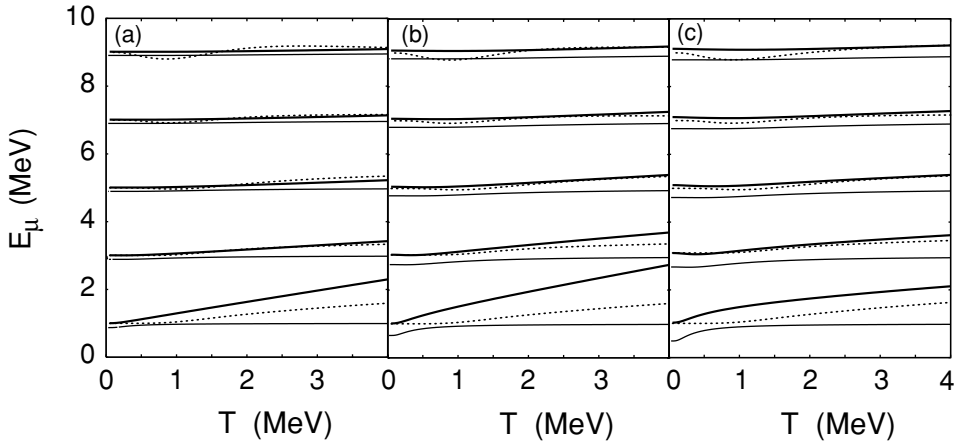


FIG. 3. Energies of the excited states $E_\mu$ of the system with $\Omega = 10$ and $N = 12$ relative to the thermal equilibrium of the system with $\Omega = N = 10$ as functions of temperature $T$. Notations are as in Fig. 2.

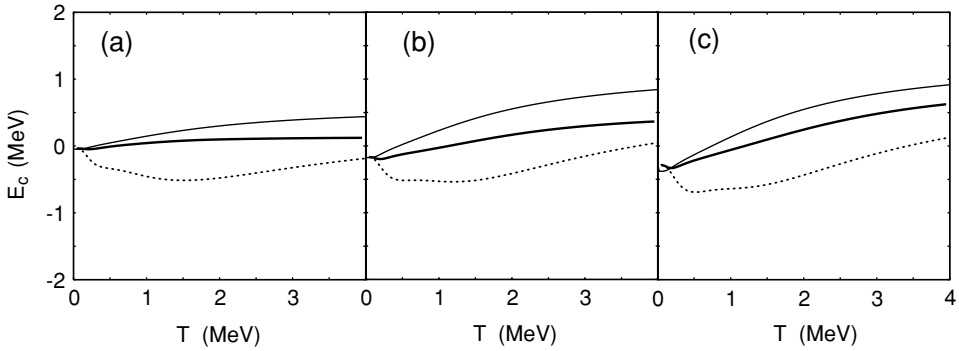


FIG. 4. Correlation energies $E_{\rm cor}$ as functions of temperature. Notations are as in Fig. 2.

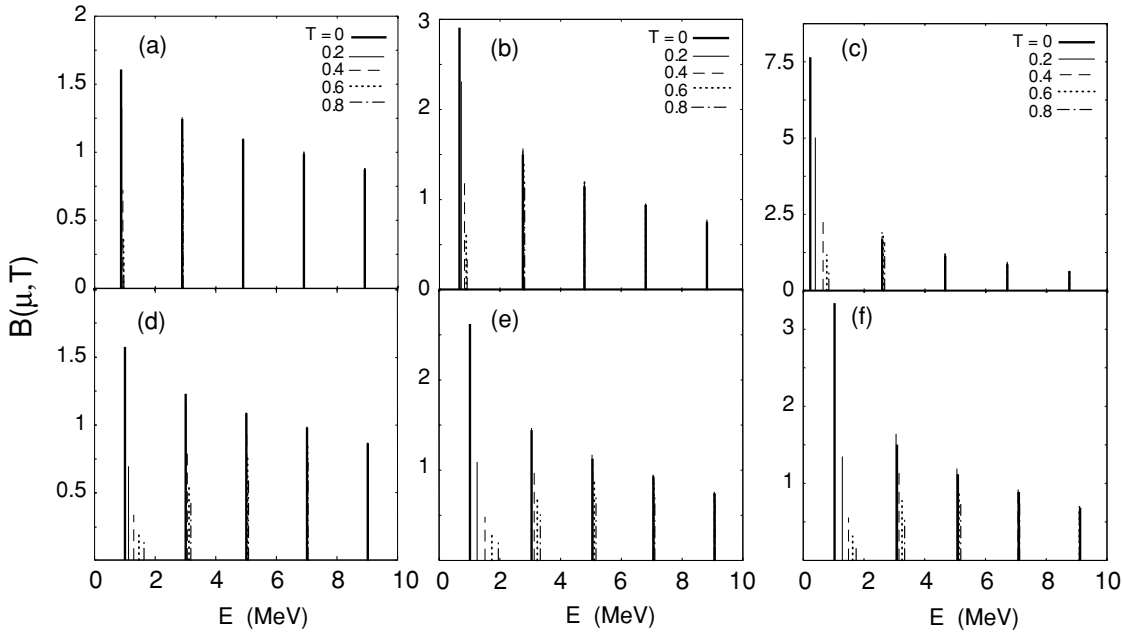


FIG. 5. Squared matrix elements $B(\mu, T)$ corresponding to the pair-transition probabilities within RPA (a)–(c) and SCRPA (d)–(f) at $T = 0.2$, 0.4, 0.6, and 0.8 MeV as indicated by the numbers next to line notations in the figure. Panel pairs (a) and (d), (b) and (e), and (c) and (f) correspond to the results obtained at $G = 0.1$, 0.2, and 0.25 MeV, respectively.

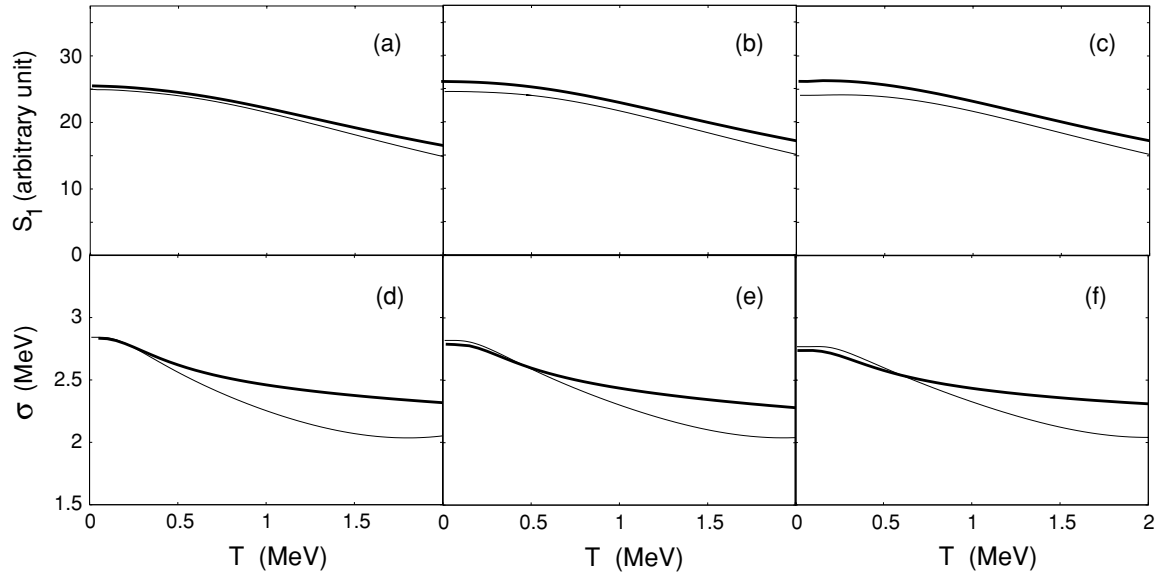


FIG. 6. EWSS $S_1$ (65) (a)–(c) and Landau splitting $\sigma$ (66) (d)–(f) as functions of temperature. Notations for the lines are as in Fig. 2; for the panels as in Fig. 5.

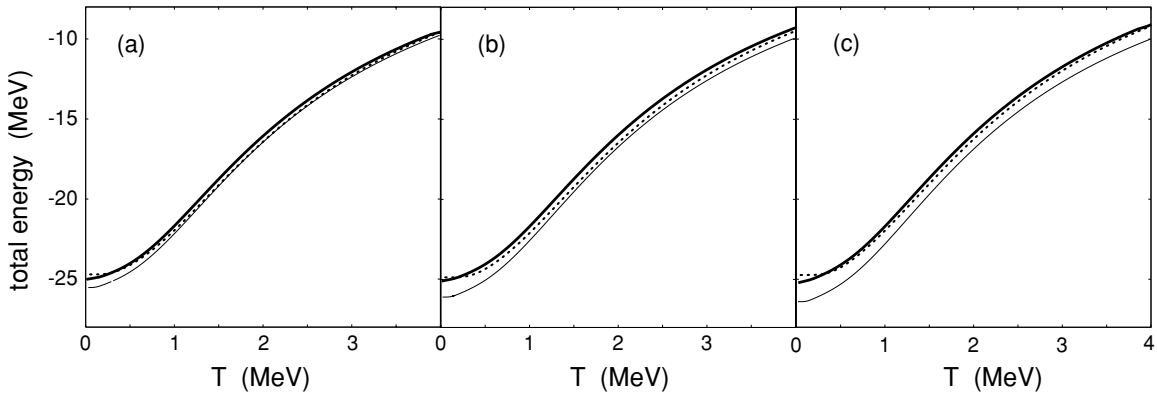


FIG. 7. Total energies $\mathcal{E}(T)$ as functions of temperature. Notations are as in Fig. 2.

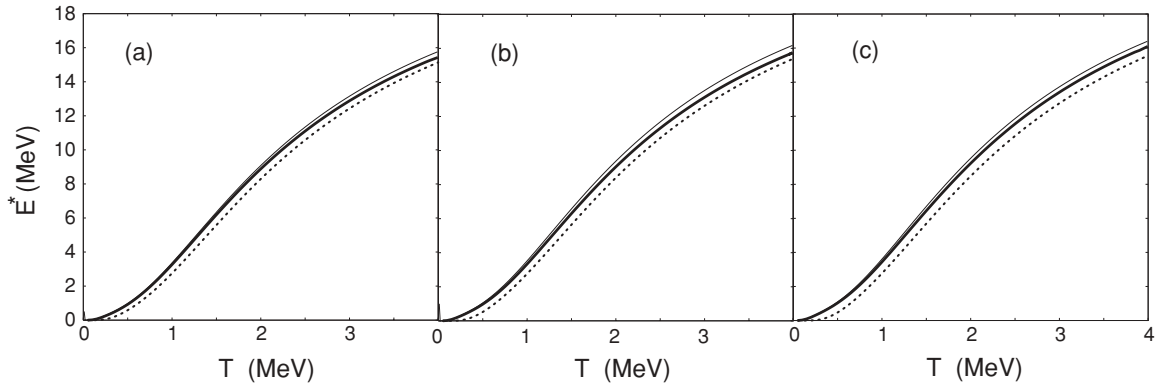


FIG. 8. Excitation energies as functions of temperature. Notations are as in Fig. 2.

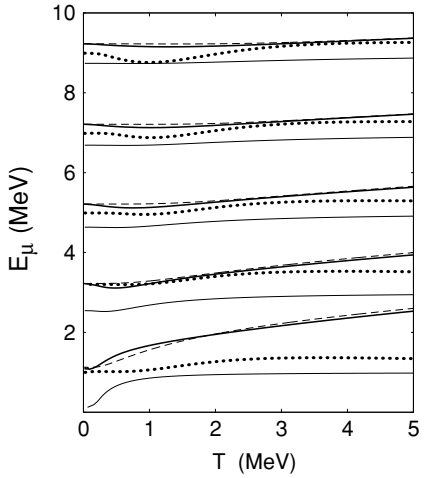


FIG. 9. Same energies $E_\mu$ as in Fig. 3 but obtained at $G = 0.33$ MeV. Dashed lines show the TSCRPA1 results of Ref. [6].

obtained within the SCRPA are slightly closer to the exact one as compared to the results obtained within the RPA.

Shown in Fig. 3 are energies $E_\mu$ of the excited states obtained within the RPA (thin lines), SCRPA (thick lines), and the exact energies (dotted lines) as functions of $T$. While the RPA energies are nearly temperature independent, the two lowest SCRPA energies ($\mu = 1$ and 2) expose a clear increase with temperature. Except for the lowest level, the SCRPA energies, in general, agree better with the exact ones. The SCRPA results are also larger than the RPA ones at all $T$, but the difference decreases at higher levels. This feature means that one can neglect the slight difference between the RPA and SCRPA in the description of collective high-lying states such as giant resonances. Meanwhile, the difference between the two approximations in the description of low-lying states, in particular, the lowest one, is quite significant and cannot be neglected, especially at high temperatures. A consequence of this effect is clearly seen in the correlation energies $E_{\rm cor}$, which are shown in Fig. 4. At $T = 0$, all the RPA, SCRPA, and exact correlation energies are close to each other. With increasing $T$, the difference starts to appear: the ascent of the RPA and SCRPA energies with $T$ becomes steeper at larger $G$. The SCRPA values always remain smaller than the RPA ones, and therefore they are closer to the exact correlation energy. The latter has an opposite curvature, which shows a decrease at low $T$ and an increase at around $T > 1.5$ MeV.

The quantities $B(\mu, T)$ obtained within the SCRPA (62) and RPA (64) at several temperatures are shown in Fig. 5. They decrease with increasing $T$. This decrease is stronger for the lower-lying states. Although the values of $B(\mu, T)$ obtained within the SCRPA are smaller than the corresponding ones given by the RPA, the larger values of the SCRPA energies $E_\mu$ lead to larger values for EWSS within SCRPA as compared to those given by the RPA, as shown in Figs. 6(a)–6(c). Both the values of EWSS obtained within RPA and SRPA decrease monotonously with increasing $T$. The Landau splitting $\sigma$ shown in Figs. 6(d)–6(f) also decreases with increasing $T$. Up to $T \sim 1.6$ MeV the decrease obtained

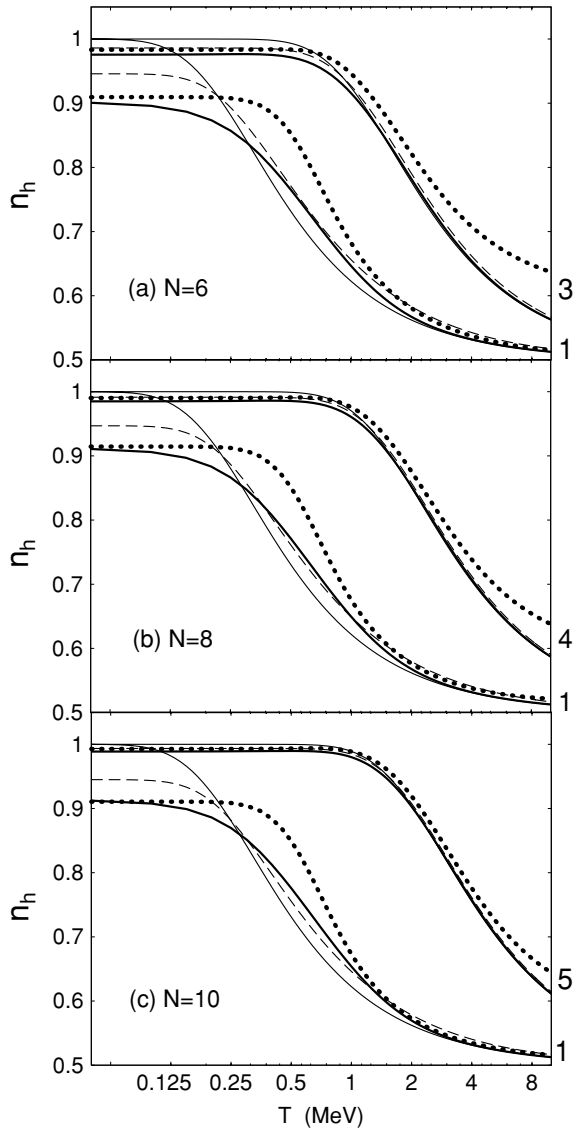


FIG. 10. Occupation numbers of the lowest and highest hole levels as functions of $T$ obtained for several particle numbers $N$ at $G \sim G_{\rm crit}^{\rm RPA}$, corresponding to each value of $N$. Notations are as in Fig. 9. The numbers at the right margin give the highest ($h = 1$) and lowest ($h = 3, 4$, and 5 for $N = 6, 8$, and 10, respectively) hole levels for which the occupation numbers are calculated.

within RPA is slightly steeper than that given by the SCRPA. The decrease of Landau splitting was seen previously in the decrease of the quantal width as the temperature increased within the phonon-damping model, which describes rather well the temperature dependence of the giant dipole resonance [20].

The total energy $\mathcal{E}(T)$ and excitation energy $E^*$ are displayed in Figs. 7 and 8, respectively, as functions of $T$. For both quantities, the SCRPA results agree better with the exact ones than do those obtained within the RPA, although the difference between them is rather small. Such a tiny difference indicates that in realistic calculations of thermodynamic quantities the conventional RPA might work reasonably well.

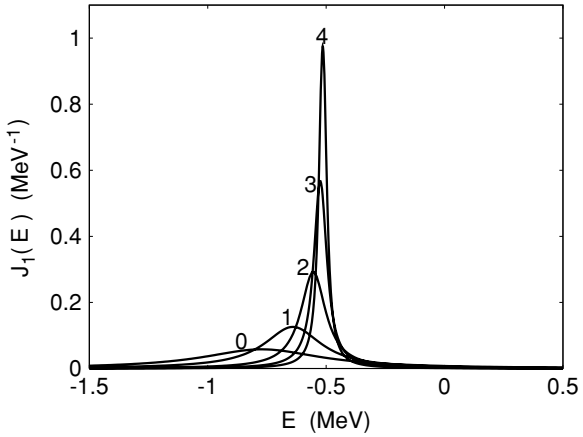


FIG. 11. Breit-Wigner-like kernel $J_1(\omega)(e^{\beta\omega}+1)$ of the spectral intensity (53) corresponding to the highest hole level for $N = 10$ and $G = 0.33$ MeV at several $T = 0$, 1, 2, 3, and 4 MeV, shown as the numbers at the peaks of the distributions. The single-particle damping $\gamma_i$ is defined as the full width at the half maximum of the distribution.

### C. Numerical comparison with the perturbative approach

In the Appendix, we analyze the formal connection between the approach developed in the present work and the TSCRPA of Ref. [6], which is based on the perturbation theory. In the present section, we compare numerically the two approaches using the results of calculations obtained at $G \simeq G^{\rm RPA}_{\rm crit}$, which are around 0.39, 0.35, and 0.33 MeV for $N = 6$, 8, and 10, respectively.

First of all, we found that the present approach and the TSCRPA give quite close energies $E_\mu$ of the addition modes. An example for $N = 10$ shown in Fig. 9 compares $E_\mu$ of the ($\Omega = 10$, $N = 12$) system, which were obtained at $G = 0.33$ MeV within our approach, the TSCRPA1, and the RPA with the exact results. At low $T$, the TSCRPA gives a slightly lower $E_1$ and higher $E_{\mu>1}$ as compared to the values obtained within our approach. However, the gap between the exact energy $E_1$ and the values offered by both of the SCRPA approaches still remains irrecoverably large and increases with $T$. The occupation numbers $n_h$ for the highest hole level, i.e., the one located just below the chemical potential, where the correlation effect is strongest, and for the lowest hole level, where this effect is weakest, are shown in Fig. 10 as functions of $T$. To magnify the difference at low $T$, the temperature axis is plotted here in the logarithmic scale. For the lowest level, the exact occupation number is close to 0.9 at $T = 0$ and remains almost constant up to $T \simeq 0.3$ MeV, then it decreases smoothly with increasing $T$. The results obtained within our approach agree very well with the exact ones at $T = 0$, where the TSCRPA overestimates them. The reason is that the single-particle damping, neglected in the TSCRPA, is rather strong as low $T$, as shown in Fig. 11. As $T$ increases, the damping gets smaller, and the occupation numbers obtained within the two approaches converge to the value given by the Fermi-Dirac distribution, which is almost the same as the exact one. There still remains a significant discrepancy in the region $0.2 \leqslant T \leqslant 1$ MeV between the exact results and those offered by both of the SCRPA approaches. For the lowest level, both approaches give results close to the Fermi-Dirac distribution. A noticeable deviation from the exact result here is seen at low $N$ and high $T$.

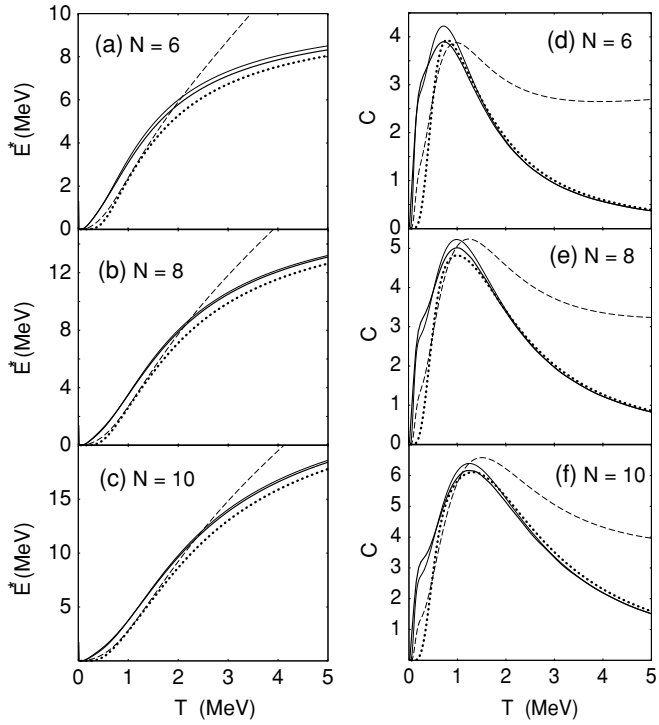


FIG. 12. Excitation energies $E^*$ in panels (a)–(c) and heat capacities $C$ in panels (d)–(f) obtained at $G = G^{\rm RPA}_{\rm crit}$ for $N = 6$, 8, and 10. Notations are as in Fig. 9.

Finally, in Fig. 12 we compare the excitation energies $E^*$ and the heat capacities $C$ obtained within our approach (thick solid lines) and the TSCRPA1 (dashed lines) with the RPA (thin solid lines) and exact results (dotted lines). The results of TSCRPA1 were obtained using Eqs. (20), (22), and (26) with $n_p$ given by Eq. (A.21) of Ref. [6]. It is seen from this figure that our approach and the RPA reproduce the overall temperature dependence of $E^*$ and $C$ given by the exact solutions at all $T$ and $N$. Moreover, the heat capacities $C$ obtained within our approach and the RPA converge to the exact values at high $T$. Meanwhile, although the TSCRPA1 reproduces rather well the exact results for $E^*$ and $C$ at $T \leqslant 2$ MeV, it fails badly to describe the exact results at $T > 2$ MeV, and the difference increases with $T$, although it slightly decreases with increasing $N$. These results demonstrate the inefficiency of the perturbative assumptions at high $T$.

## VI. CONCLUSIONS

The present paper extends the SCRPA to finite temperature, where the single-particle occupation numbers are calculated self-consistently. By using the double-time Green's functions method, the present approach is free from the constraints of the perturbation theory. The analytic properties of the double-

time Green's functions allow the calculations of the single-particle damping to be carried out in a straightforward manner. The calculations performed within the Richardson model show that, except for the lowest-energy level, the results obtained within the SCRPA are rather similar to those given by the RPA, where the occupation numbers are approximated by the Fermi-Dirac distribution for noninteracting fermions. As compared to the RPA, the SCRPA offers a slightly better agreement with the exact solutions for the thermodynamic quantities such as the total energy, excitation energy, and heat capacity. The difference from 1 (0) for the hole (particle) occupation numbers obtained at $T \sim 0$ within the SCRPA due to the ground-state correlations beyond RPA does not affect significantly the integrated quantities obtained within the RPA such as the EWSS and Landau splitting. This indicates that in realistic calculations for high-lying states such as giant resonances, the conventional RPA at finite temperature might be sufficient and more convenient than the computationally expensive SCRPA. For the first excited states, however, care should be taken, particularly for light systems at the large interaction strength, to ensure that the correlation effects are properly included.

Last but not least, it is worth noting that the exact solutions of a system with pure pairing do not represent a full thermalization. The seniority conservation prevents a number of particles to interact with each other. As a result, for the exact solutions, the temperatures defined in different ways do not agree [21]. Moreover, occupation numbers generally do not show a Fermi-Dirac distribution. However, in realistic nuclei, seniority is broken and residual interactions, no matter how weak they are, immediately thermalize the systems, as has been the case in the full shell model [22]. This is the reason why the statistical approach to highly excited nuclei has become so good. This also explains why one should not expect a perfect agreement between the exact solutions and those given by the RPA or SCRPA approaches. Furthermore, since the exact solutions to the pairing problem describe an unphysical and poorly thermalized situation at $T \neq 0$, which clearly lacks the effect of particle-particle collisions in a nonpairing channel, the FT-SCRPA is the preferred lowest-order approach for applications in realistic systems at finite temperature. This approach still uses the pairing Hamiltonian to drive the dynamics, but imposes the thermalization conditions on unpaired particles to mimic the small and generally random contributions of nonpairing residual interactions. More elaborated approaches should include higher-order effects, which are beyond the SCRPA, such as couplings to configurations more complicated than *ph*, *pp*, and *hh* ones.

## ACKNOWLEDGMENTS

The authors are grateful to Alexander Volya (Florida State University) for help in the exact solutions of the Richardson model and for fruitful discussions as well as valuable suggestions in revising the manuscript. The use of the FORTRAN IMSL Library by Visual Numerics on the RIKEN Super Combined Cluster (RSCC) System is also acknowledged.

## APPENDIX A: PERTURBATIVE APPROACH AS LIMITING CASE FOR SMALL SINGLE-PARTICLE DAMPING

The perturbative approach (TSCRPA) of Ref. [6] is based on two assumptions: (1) the omission of the single-particle damping (the imaginary part of the mass operator) and (2) the additional consistency condition. These assumptions are analyzed below in connection with the approach of the present work.

### 1. Limit of very small single-particle damping

We have seen that our approach allows us to derive the explicit form (49) for the single-particle Green's function without assuming any perturbation expansion. As a matter of fact, the Green's function in (49) can be expanded in a power (Maclaurin) series of $\Phi(E)$ as

$$G_i(E) = G_i^0(E) - G_i^0(E)\Phi_i(E)G_i^0(E) + G_i^0(E)\Phi_i(E)G_i^0(E)\Phi_i(E)G_i^0(E) - \ldots, \quad \text{(A1)}$$

with the unperturbed single-particle Green's function $G_i^0(E) = [2\pi(E - \epsilon_i + \lambda)]^{-1}$. The diagrammatic representation of Eq. (A1) is depicted in Fig. 13. Depending on the assumption of the smallness of $|\Phi_i(E)|$, one may cut this series at the term $\sim O(|\Phi_i(E)|^n)$ with a definite $n$. If $|\Phi_i(E)|$ is so small that only the first order ($n = 1$) can be kept, Eq. (A1) is formally reduced to the truncation scheme (27) of Ref. [6]. The approximation scheme considered here is, therefore, more general than that used in Ref. [6]. Consequently, Eq. (59) is formally exact up to the mass operator $\Phi_i(\omega)$ and the damping $\gamma_i(\omega)$. No assumption on the smallness of $\gamma_i(\omega)$ nor perturbation expansion in power series of $\omega$ was made in Eq. (59). The explicit expression (55) for single-particle damping is the major advantage of the present approach, because the double-time Green's functions method allows the mass operator (50) to be analytically continued into the complex-energy plane. The imaginary part of such continuation yields the damping (55). This is not possible within the method based on the perturbation theory [6], since the causal Green's functions used in the latter do not allow such continuation.

In the limiting case of very small damping $\gamma_i(\omega)$ (55), the spectral intensity $J_i(\omega)$ (53) has a steep maximum at a certain value $\omega = \widetilde{\epsilon}_i$, which is defined as the pole of the Green's function (49), i.e., the solution of the equation

$$\widetilde{\epsilon}_i = \epsilon_i - \lambda - \Phi(\widetilde{\epsilon}_i). \quad \text{(A2)}$$

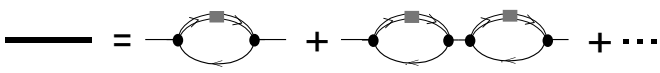

FIG. 13. Summation of diagrams in Eq. (A1). A right-arrow double line denotes a (forward-going) particle (hole) pair with energy $2\epsilon_j$, while a left-arrow single line stands for a (backward-going) particle (hole) with energy $\epsilon_i$. A thin horizontal line represents the unperturbed Green's function $G_i^0(E)$. A bubble denotes the mass operator $\Phi_i(E)$, and a gray rectangle represents $\mathcal{M}_j$ (47). The thick solid line stands for the full Green's function $G_i(E)$.

In this case, following Ref. [9], we can expand the mass operator $\Phi_i(\omega)$ (50) in power series of $\omega$ near this value. As a result, we obtain

$$J_i(\omega) \simeq \frac{1}{\pi} \frac{\left[1 + \left(\frac{d\Phi_i}{d\omega}\right)_{\omega=\widetilde{\epsilon}_i}\right]^{-1} \widetilde{\gamma}_i(\widetilde{\epsilon}_i)(e^{\beta\omega}+1)^{-1}}{(\omega - \widetilde{\epsilon}_i)^2 + \widetilde{\gamma}_i^2(\widetilde{\epsilon}_i)}, \quad \text{(A3)}$$

where

$$\widetilde{\gamma}_i(\widetilde{\epsilon}_i) = \gamma_i(\widetilde{\epsilon}_i)\left[1 + \left(\frac{d\Phi_i}{d\omega}\right)_{\omega=\widetilde{\epsilon}_i}\right]^{-1}, \quad \text{(A4)}$$

under the assumption that

$$\left|\frac{d\Phi_i}{d\omega}\right|_{\omega=\widetilde{\epsilon}_i} \ll 1, \quad \text{(A5)}$$

i.e., $\widetilde{\gamma}(\widetilde{\epsilon}_i)$ plays the role of the damping of the elementary excitation with a renormalized energy $\widetilde{\epsilon}_i$ given by Eq. (A2). For very small values of $\widetilde{\gamma}_i$, replacing the Breit-Wigner-like kernels $\widetilde{\gamma}_i(\widetilde{\epsilon}_i)/\{(\omega - \widetilde{\epsilon}_i)^2 + \widetilde{\gamma}_i^2(\widetilde{\epsilon}_i)\}$ in $J_i(\omega)$ with the $\delta$ functions using Eq. (58), we get from (59)

$$\begin{aligned} n_i &\simeq \int_{-\infty}^{\infty} \frac{\delta(\omega - \widetilde{\epsilon}_i)}{\left[1 + \left(\frac{d\Phi_i}{d\omega}\right)_{\omega=\widetilde{\epsilon}_i}\right]^{-1}(e^{\beta\omega}+1)} d\omega \\ &\simeq \int_{-\infty}^{\infty} \frac{\delta(\omega - \widetilde{\epsilon}_i)\left[1 - \left(\frac{d\Phi_i}{d\omega}\right)_{\omega=\widetilde{\epsilon}_i}\right]}{e^{\beta\omega}+1} d\omega \\ &= \widetilde{n}_i - \int_{-\infty}^{\infty} \frac{\left(\frac{d\Phi_i}{d\omega}\right)_{\omega=\widetilde{\epsilon}_i}\delta(\omega - \widetilde{\epsilon}_i)}{e^{\beta\omega}+1} d\omega, \end{aligned} \quad \text{(A6)}$$

where $\widetilde{n}_i \equiv (e^{\beta\widetilde{\epsilon}_i}+1)^{-1}$ are the occupation numbers of the free (but renormalized) single-particle states, whose Green's functions are given as

$$\widetilde{G}_i(E) = \frac{1}{2\pi}\frac{1}{E - \widetilde{\epsilon}_i} \quad \text{(A7)}$$

instead of (49). The expansion at the rhs of Eq. (A6) is formally the same as that given by Eq. (32) or (A.21) of Ref. [6]. The difference is in the explicit expression mass operator $\Phi_i(\omega)$, which leads to the difference in the last term at the rhs of Eq. (A6).[2] One can see that because of the finite imaginary part (finite damping), the singularities of the single-particle Green's function (49) on the real-energy axis are not the poles. Only the approximate Green's function, where the damping is neglected, has poles on the real axis, which determine the energy $\widetilde{\epsilon}_i$ (A2) of (undamped) elementary excitations.

[2]As $\Phi_i(\omega)$ belongs to the Fourier transform of the retarded single-particle Green's function, it cannot be compared directly with Eq. (28) of Ref. [6], which comes from the Fourier transform of the lowest order in the perturbation expansion of the causal Green's function. For noninteracting single particles, e.g., the Fourier transform of the causal Green's function is given as $G_j^c(E) = [(1 - n_j^{\rm FD})G_j^r(E) + n_j^{\rm FD}G_j^a(E)]$, where $G_j^r(E) = (2\pi)^{-1}(E - \epsilon_j + i\varepsilon)^{-1}$, and $G_j^a(E) = (2\pi)^{-1}(E - \epsilon_j - i\varepsilon)^{-1}$ are temperature-independent Fourier transforms of retarded and advanced Green's functions, respectively.

### 2. Additional consistency condition

Strictly speaking, a fully consistent use of Eq. (23.15) of Ref. [23], which relates the expectation value of the model Hamiltonian to the single-particle causal Green's functions, only takes place if one neglects the last term at the rhs of (A6) under the assumption (A5). In this case, $n_i \simeq \widetilde{n}_i$ and the model Hamiltonian can be approximated as

$$H \simeq \sum_i \widetilde{\epsilon}_i N_i. \quad \text{(A8)}$$

Using the definitions (36) and (37), we relate the retarded single-particle Green's function (39) to the causal one in Ref. [23] as

$$G_i(t - t') = G_i^c(t - t') - i[\theta(t - t') + \theta(t' - t)]\mathcal{F}_i(t - t'). \quad \text{(A9)}$$

As the time-correlation function $\mathcal{F}_i(t - t')$ satisfies the equation $id\mathcal{F}_i/dt = \langle c^\dagger(t')[a_i(t), H(t)]\rangle$ and since $d\theta(t' - t)/dt = -d\theta(t - t')/dt$, it follows that, with Hamiltonian (A8), the Green's function in (39) also satisfies Eq. (23.15) of Ref. [23], which is referred to as Eq. (25) in Ref. [6].

Because the perturbative approach of Ref. [6] used Eq. (A6) including the integral term, it goes beyond the consistency mentioned above. Therefore, an additional consistency condition was introduced. This condition requires that the total energies obtained from Eq. (25) of Ref. [6] and those obtained by calculating the expectation value of the Hamiltonian including the original two-body Green's functions in Eq. (26) of Ref. [6] are the same. However, as has already been pointed out in Ref. [6], this is possible only if, apart from the assumption of very small damping discussed above, the expansion (A1) of the Green's function (49) is truncated to the first order in the renormalized single-particle mass operator, i.e., one has to use

$$\begin{aligned} G_i(E) &\equiv G_i^0(E)[1 + \Phi_i(E)G_i^0(E)]^{-1} \\ &\simeq G_i^0(E)[1 - \Phi_i(\widetilde{\epsilon}_i)G_i^0(E)] \end{aligned} \quad \text{(A10)}$$

instead of the full single-particle Green's function (49). Generally speaking, this recipe is legitimate and, in principle, desirable because it follows the standard perturbative treatment of the mass operator as has been used in the particle-vibration coupling [24] or hole-pair vibration coupling considered here. However, in the present case within the SCRPA, a complete application of this recipe is not as simple as using the exact expression (68) to calculate $\mathcal{E}(T)$. The reason is that in following this recipe, the single-particle energies $\widetilde{\epsilon}_i$ (A2) need to be renormalized again so that the resulting renormalized Green's function can describe the propagation of noninteracting newly renormalized single particles with energies $\widetilde{\epsilon}'_i \neq \widetilde{\epsilon}_i$, taking into account also the integral term at the rhs of Eq. (A6). Only in this case one can properly represent the final Hamiltonian in the form (A8) (with $\widetilde{\epsilon}'_i$ replacing $\widetilde{\epsilon}_i$) in order to fully satisfy the consistency condition of Eq. (23.15) of Ref. [23]. Obviously, the renormalized energies $\widetilde{\epsilon}_i$ and $\widetilde{\epsilon}'_i$ are already much more complicated than the single-particle energy $\epsilon_k$ given by Eqs. (30) or (A.19) of Ref. [6], let alone the newly renormalized energies $\widetilde{\epsilon}'_i$. This means that such a renormalization effect is missing in Ref. [6]. The crucial

consequence of this is seen in the final expression (26) in Ref. [6] for the total energy $\mathcal{E}(T)$, which can be rewritten after expressing $F_\mu$ in terms of $X_p^\mu$ using Eq. (20a) therein as

$$\mathcal{E}^{\mathrm{TSCRPA}}(T) = -\frac{\Omega^2}{4} + 2\sum_p(\epsilon_p - \lambda)(1 - \langle D_p\rangle) - 2\sum_{p,\mu}(|C_p| - E_\mu)X_p^\mu\left[\nu_\mu X_p^\mu + (1+\nu_\mu)Y_p^\mu\right]. \tag{A11}$$

This result is different from the exact expression (68) for $\mathcal{E}(T)$. Indeed, the leading orders of the last term at the rhs of Eq. (A11) are $O[(X_p^\mu)^2]$ and $O[X_p^\mu Y_p^\mu]$, while the exact expression (68), apart from these terms, also contains the terms of order $O[(Y_p^\mu)^2]$, which are not small when $G$ is close to $G_{\mathrm{crit}}^{\mathrm{RPA}}$. As the approach of the present work solves the full single-particle Dyson equation starting from the equation of motion (38) for the double-time Green's functions without any perturbative treatment of the mass operator, it is free from such additional consistency condition. Moreover, when the temperature is sufficiently high, higher orders in the perturbative expansion become important, which invalidate the applicability of the first-order theory including the above-mentioned additional consistency condition. Therefore, as it is often done within the SCRPA to calculate the ground-state energy, we prefer to use the exact expression (68) to calculate the energy $\mathcal{E}(T)$ because not only is it simple but also it yields better results within a larger temperature region.


[1] A. V. Ignatyuk, *Statistical Properties of Excited Atomic Nuclei* (Energoatomizdat, Moscow, 1983); M. H. Sommermann, Ann. Phys. (NY) **151**, 163 (1983); D. Vautherin and N. Vinh Mau, Nucl. Phys. **A422**, 140 (1984); N. Dinh Dang, J. Phys. G **11**, 125 (1985); K. Tanabe and K. Sugawara-Tanabe, Phys. Lett. **B172**, 129 (1986); N. Dinh Dang, Z. Phys. A **335**, 253 (1990); K. Tanabe and N. D. Dang, Phys. Rev. C **62**, 024310 (2000).

[2] K. Hara, Prog. Theor. Phys. **32**, 88 (1964); K. Ikeda, T. Udagawa, and H. Yamamura, *ibid.* **33**, 22 (1965); D. J. Rowe, Phys. Rev. **175**, 1283 (1968); P. Schuck and S. Ethofer, Nucl. Phys. **A212**, 269 (1973); F. Catara, N. D. Dang, and M. Sambataro, *ibid.* **A579**, 1 (1994).

[3] J. Dukelsky and P. Schuck, Nucl. Phys. **A512** 466, (1990); J. Dukelsky, G. Roepke, and P. Schuck, *ibid.* **A628**, 17 (1998).

[4] J. Dukelsky and P. Schuck, Phys. Lett. **B464**, 164 (1999).

[5] J. G. Hirsch, A. Mariano, J. Dukelsky, and P. Schuck, Ann. Phys. (NY) **296**, 187 (2002).

[6] A. Storozhenko *et al.*, Ann. Phys. (NY) **307**, 308 (2003).

[7] M. Schmidt, G. Röpke, and H. Shulz, Ann. Phys. (NY) **202**, 57 (1990).

[8] N. N. Bogolyubov and S. V. Tyablikov, Sov. Phys. Dokl. **4**, 60 (1959) [Dokl. Akad. Nauk SSSR **126**, 53 (1959)].

[9] D. N. Zubarev, Sov. Phys. Usp. **3**, 320 (1960) [Usp. Fiz. Nauk **71**, 71 (1960)].

[10] A. Volya, B. A. Brown, and V. Zelevinsky, Phys. Lett. **B509**, 37 (2001).

[11] N. D. Dang, Phys. Rev. C **71**, 024302 (2005).

[12] N. Dinh Dang, Eur. Phys. J. A. **16**, 181 (2003).

[13] R. W. Richardson, Phys. Lett. **3**, 277 (1963); **5**, 82 (1963); **14**, 325 (1965).

[14] F. Pan, J. P. Draayer, and W. E. Ormand, Phys. Lett. **B422**, 1 (1998).

[15] A. Bohr and B. R. Mottelson, *Nuclear Structure* (Benjamin, New York, 1969), Vol. I.

[16] S. Y. Tsay Tzeng, P. J. Ellis, T. T. S. Kuo, and E. Osnes, Nucl. Phys. **A580**, 277 (1994).

[17] R. Kubo, M. Toda, and N. Hashitsume, *Statistical Physics II: Nonequilibrium Statistical Mechanics* (Springer, Heidelberg, 1985), pp. 223, 224.

[18] O. Civitarese, G. G. Dussel, and A. P. Zuker, Phys. Rev. C **40**, 2900 (1989); J. Dukelsky, A. Poves, and J. Retamosa, *ibid.* **44**, 2872 (1991); O. Civitarese and M. Schvellinger, *ibid.* **49**, 1976 (1994).

[19] R. K. Bhaduri and W. Van Dijk, Nucl. Phys. **A485**, 1 (1988); H. G. Miller, B. J. Cole, and R. M. Quick, Phys. Rev. Lett. **63**, 1922 (1989).

[20] N. D. Dang and A. Arima, Phys. Rev. Lett. **80**, 4145 (1998); N. Dinh Dang and A. Arima, Nucl. Phys. **A636**, 427 (1998); N. D. Dang, K. Tanabe, and A. Arima, Phys. Rev. C **58**, 3374 (1998); N. Dinh Dang, K. Tanabe, and A. Arima, Nucl. Phys. **A645**, 536 (1999).

[21] V. Zelevinsky and A. Volya, Phys. Part. Nucl. **66**, 1829 (2003).

[22] V. Zelevinsky, B. A. Brown, N. Frazier, and M. Horoi, Phys. Rep. **276**, 85 (1996).

[23] A. L. Fetter and J. D. Walecka, *Quantum Theory of Many-Particle Systems* (McGraw-Hill, New York, 1971).

[24] A. Bohr and B. R. Mottelson, *Nuclear Structure* (Benjamin, New York, 1975), Vol. II.